J Porous Mater (2012) 19:295–300
DOI 10.1007/s10934-011-9475-8

Synthesis, characterization and phenol adsorption of carbonyl-functionalized mesoporous silicas

Phuong Tran Thi Thu · Hang Tran Dieu · Hung Nguyen Phi · Nga Nguyen Thi Viet · Sung Jin Kim · Vien Vo

Published online: 8 May 2011

Abstract Carbonyl-functionalized mesoporous silicas have been synthesized by co-condensation of tetraethoxysilane and varying contents of 3-(trimethoxysilyl)propyl methacrylate in acidic medium with the block copolymer Pluronic 123 as a structure directing agent. The functionalized materials were characterized by PXRD, TEM, SEM, IR, and N_2 adsorption–desorption at 77 K. Adsorption of phenol in aqueous solution on the materials has been investigated. The experimental results showed that carbonyl-functionalized mesoporous silicas possess strong adsorption ability for phenol with interaction of O-H…O = C hydrogen bond. The adsorption data are fitted to Langmuir Isotherms and a maximum adsorption capacity calculated from the Langmuir equation can reach 0.87 mmol of phenol/g. The effect of the pH on phenol adsorption has been studied.

Keywords Mesoporous materials · Functionalization · Methacrylate · Phenol adsorption

1 Introduction

The rapid growth of the chemical and petrochemical industries may lead to pollute surface and ground water and air by various inorganic and organic chemicals. Among organic compounds, phenol and its derivatives are classified as highly toxic, harmful to living organisms even at low concentrations. Phenol-contained wastewater brings a series of serious environmental problem due to its high toxicity and accumulation in the environment [1]. Phenols have entered the environment by the way of various industrial processes, such as oil refining, petrochemical production, ceramic manufacturing, coal conversion and the phenolic resin industry [2]. There are many traditional methods to remove phenols from aqueous solutions: adsorption, chemical oxidation, precipitation, distillation, solvent extraction, ion exchange, membrane processes, and reverse osmosis [3]. Among these, adsorption has significant advantages, including high efficiency, ease of handling, high selectivity, low operating costs, easy regeneration of adsorbent, and minimal generation of chemical or biological sludge [4]. There are experimental studies on phenol adsorption by activated carbon [5], red mud [6] and rubber seed coat [7], clay minerals [8], and other methods. Adsorption process is strongly affected by the chemistry and surface morphology of the adsorbent. Therefore, new adsorbents, which are economical, having strong affinity and high loading capacity have been required.

In 1998, Stucky and co-workers reported a new class of mesoporous materials synthesized at low pH and with neutral templates [9]. The hexagonally ordered material with large pore diameters and wall thicknesses of this class was called SBA-15. Furthermore, the structure directing agents used for the synthesis of these materials (triblock copolymer poly(ethylene oxide)-poly(propylene oxide)-poly(ethylene oxide) type) are not expensive, nontoxic, and biodegradable [10]. Therefore, the structural characteristics of SBA-15 make it an interesting material for adsorption and catalytic applications. Recently, the design of mesostructured-based adsorbents for the removal of toxic heavy-metal ions from

P. T. T. Thu · H. T. Dieu · H. N. Phi · N. N. T. Viet · V. Vo (✉)
Department of Chemistry, Quy Nhon University, 170 An Duong Vuong, Quy Nhon, Binh Dinh, Vietnam
e-mail: vovien@qnu.edu.vn

S. J. Kim
Department of Chemistry and Nano Sciences, Ewha Womans University, Seoul 120-750, Korea

aqueous solutions is a subject that has been intensively investigated [11, 12]. For this purpose, a variety of organic functional groups such as thiol, amine can be grafted or incorporated onto the surface of SBA-15 mesopore channels using ligand-functionalized organosilanes [13, 14]. However, few papers have been reported on functionalized ordered-mesophase materials for adsorption of organic compounds from water [15]. In this work, for the first time, we present the synthesis of carbonyl-functionalized SBA-15 materials using varying proportions of 3-(trimethoxysilyl)propyl methacrylate as a carbonyl source through one-pot synthesis, and the phenol adsorption on the functionalized materials.

2 Experimental section

2.1 Chemical

Triblock copolymer Pluronic P123 ($HO(CH_2CH_2O)_{20}(CH_2CH(CH_3)O)_{70}(CH_2CH_2O)_{20}H$), tetraethyl orthosilicate ($(C_2H_5O)_4Si$) and 3-(trimethoxysilyl)propyl methacrylate ($CH_2 = C(CH_3)COO(CH_2)_3Si(OCH_3)_3$) were purchased from Merck. Hydrochloric acid (HCl) was purchased from Shanghai Chemical Company. All chemical were used as received without any further purification.

2.2 Synthesis

Carbonyl-functionalized SBA-15 samples were synthesized by the following procedure. 2 g of P123 were added to 62.5 g of HCl 1.9 M with stirring. The mixture was heated to 40 °C and then to the mixture 3.84 g of etraethoxysilane (TEOS) was added. The resulting mixture was stirring for 2 h and then 3-(trimethoxysilyl)propyl methacrylate (TSPM) was added to the mixture. Three different molar ratios of TSPM/(TEOS + TSPM) of 0.05, 0.07, and 0.10 were used in three initial mixtures, individually. The reaction mixture was stirred for 20 h at 40 °C, and then aged in an autoclave at 100 °C for 24 h. The solid product was separated by filtration, and washed with water several times. The structure directing agent (P123) was removed by using ethanol extraction at 70 °C for 24 h. These obtained materials are denoted as SBA-15/CO-x, where x is referred as the molar ratio of TSPM/(TEOS + TSPM) in percentage in the initial mixture.

2.3 Characterization

X-ray diffraction (XRD) for the samples were measured on the Brucker D8 Advance diffractometer using CuKα radiation ($\lambda = 1.5406$ Å). N_2 adsorption–desorption isotherms were obtained on ASAP 2010 at 77 K. Before the measurement, the samples were degassed at 100 °C for 6 h. Infrared (IR) absorption spectra for the samples were recorded on a Thermo Nicolet spectrometer. Transmission electron microscopy (TEM) and scanning electron microscopy (SEM) images were recorded on JEOL JEM-2100F and JEOL 5410, respectively.

2.4 Phenol adsorption

We carried out different sets of batch experiments to investigate the effect of the adsorption of phenol on contact time, the initial phenol concentration, and the pH of the aqueous solution. Single runs were carried out by stirring 50 mg of the adsorbent in 20 mL of aqueous phenol solution at 30 °C. When the adsorption procedure was completed, the adsorbents were separated through centrifugation. The concentration of the remaining phenols in the supernatant was determined through UV absorption spectroscopy (absorption λ max at 269 nm) with a SCINCO S-4100 PDA UV-Vis spectrophotometer. The phenol adsorption capacity was determined by the difference between the initial and final phenol concentrations in the solution. The influence of pH on the adsorption property of SBA-15/CO-x was examined by varying the pH of each solution with NaOH and HCl solutions. The pH was measured with a pH meter (pH-200 L, NEOMET).

3 Results and discussion

3.1 Characterization of adsorbents

The porous structure of the synthesized samples has been studied by low-angle XRD. The patterns in Fig. 1 show an intense reflection (100) and one additional weak peak at higher angle (110) for SBA-15/CO-5 and SBA-15/CO-7, indicative of a 2-D hexagonal space group with high p*6 mm* symmetry [9]. The sample containing the highest TSPM ratio in the initial mixture, SBA-15/CO-10 exhibits a single reflection with a significant intensity decrease and peak broadening. These results can be attributed to the loss of mesostructured order of the material with increasing propyl methacrylate content. From these values, the hexagonal lattice parameters are calculated and reported in Table 1. The pore size and periodicity in the mesostructure of SBA-15/CO-x materials were confirmed directly by transmission electron microscopy. The TEM image for a representative material, SBA-15/CO-10 exhibits a highly ordered hexagonal arrangement of mesopores (Fig. 2). Both the perpendicular and parallel channels relative to the longitudinal axis are observed. The approximate interpore spacing of 9 nm is close to the value calculated from the XRD pattern, $a_0 = 8.9$ nm. The pore size and wall

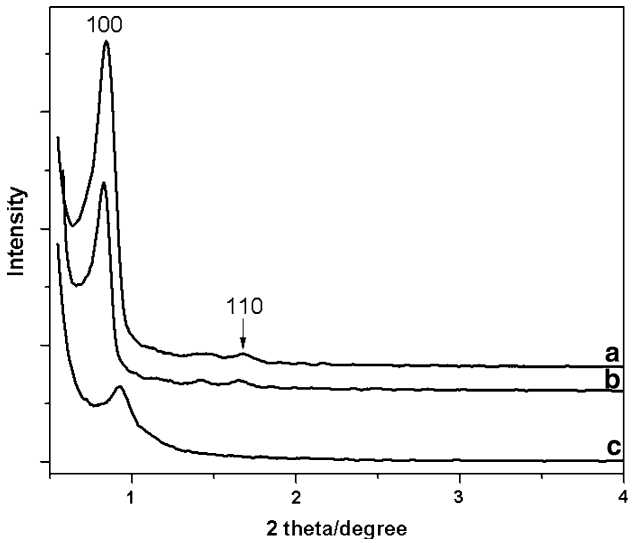

Fig. 1 Powder low-angle XRD patterns of the carbonyl-modified SBA-15 materials: SBA-15/CO-5 (*a*), SBA-15/CO-7 (*b*), and SBA-15/CO-10 (*c*)

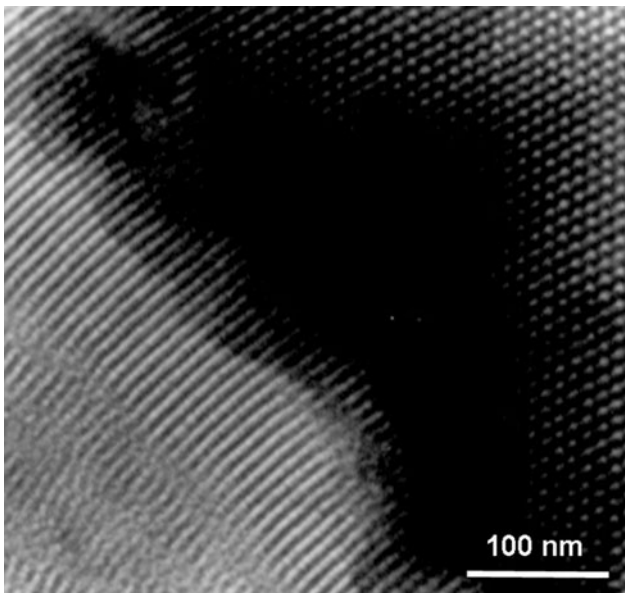

Fig. 2 TEM image of SBA-15/CO-10

thickness, estimated from the HR-TEM image, are approximately 5.0 and 4.0 nm, respectively. The morphology of rope-like domains with an uniform size has been obtained for all the materials. The size of 0.5 μm in diameter of rope-like domains for a representative sample, SBA-15/CO-10 can be seen from the image (Fig. 3).

The N_2 adsorption/desorption isotherms at 77 K as well as the calculated pore size distributions of carbonyl-functionalized SBA-15 samples are shown in Fig. 4. Characteristic mesoporous type IV IUPAC isotherms have been found for all samples. For the functionalized SBA-15 samples, it has been shown that isotherms with a capillary condensation of N_2 occurred over a slightly lower P/P_0 range and a slightly smaller pore volume in the functionalized samples with higher content of propyl methacrylate. Generally, a change in the shape of isotherms and a broadening of the pore size distribution are observed when carbonyl functionalization increases. Pore diameter, pore volume, and superficial area BET (S_{BET}) are also found to decrease significantly with increasing propyl methacrylate group content. Conversely, silica wall thickness extracted from the XRD and nitrogen sorption parameters steadily increases in the same order (Table 1). These results can be attributed to the occupancy of methacrylate groups into the mesostructure. The above physisorption data indicate the presence of carbonyl groups, and the textural properties of SBA-15 were significantly maintained, showing a suitable porosity to act as adsorbents.

The incorporation of carbonyl groups into the silicate frameworks can be qualitatively confirmed by the FTIR data. FTIR spectra of three functionalized SBA-15 samples are illustrated in Fig. 5. For comparison, also shown in the figure are the spectra of P123 and SBA-15 calcined at 550 °C for removing P123. For P123, the absorbance peaks corresponding to the C-H stretching and bending vibrations appear in the range of 2,850–3,000 and 1,460 cm^{-1}, respectively. Those at 1,377 and 1,350 cm^{-1} are assigned to the stretching modes of C–O–C on P123 [16]. These peaks became negligible on the extracted SBA-15/CO-10 material, indicating that the surfactant in the extracted materials was almost completely removed upon extraction with ethanol. It is worth to note that a shoulder around 1,697 cm^{-1} appearing in all spectra of the three samples SBA-15/CO-5, SBA-15/CO-7 and SBA-15/CO-10 may correspond to vibrational mode of C = O group [17, 18]. The intensity of this shoulder increases with increasing content of TSPM in the initial mixture. These results evidence strongly that the carbonyl groups are present in the functionalized materials and the carbonyl contents in the

Table 1 Structural, textural properties of the carbonyl-funtionalized SBA-15 materials

Material	S_{BET} (m^2/g)	Pore diameter (nm)	a_o (nm)	Wall thickness (nm)
SBA-15/CO-5	512.7	5.7	9.1	3.4
SBA-15/CO-7	414.2	5.5	9.3	3.8
SBA-15/CO-10	300.3	4.9	8.9	4.0

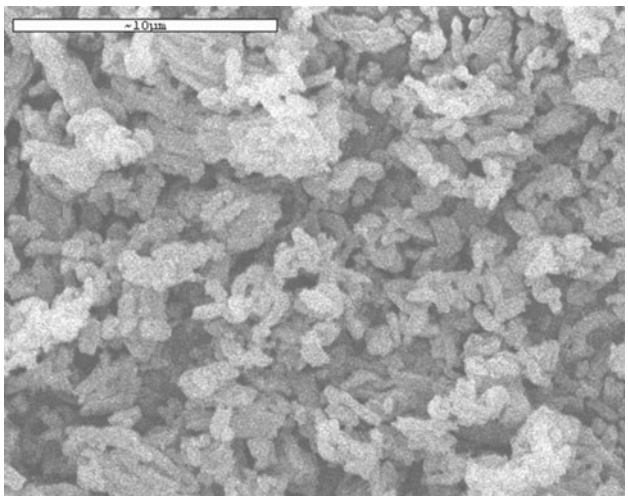

Fig. 3 SEM image of SBA-15/CO-10

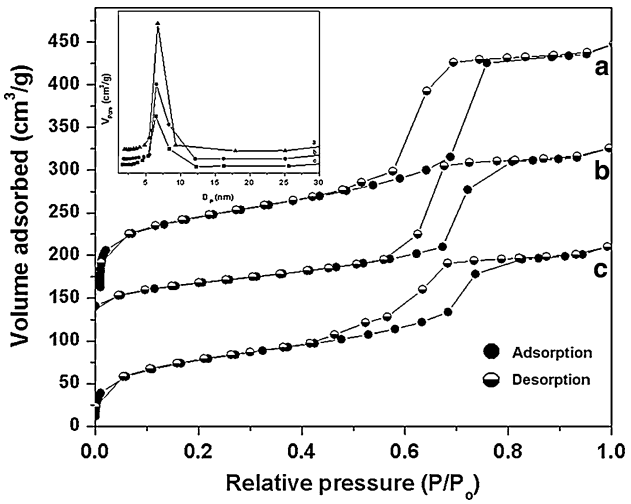

Fig. 4 N_2 adsorption–desorption isotherms and pore size distribution curves (the inset) of SBA-15/CO-5 (*a*), SBA-15/CO-7 (*b*), and SBA-15/CO-10 (*c*)

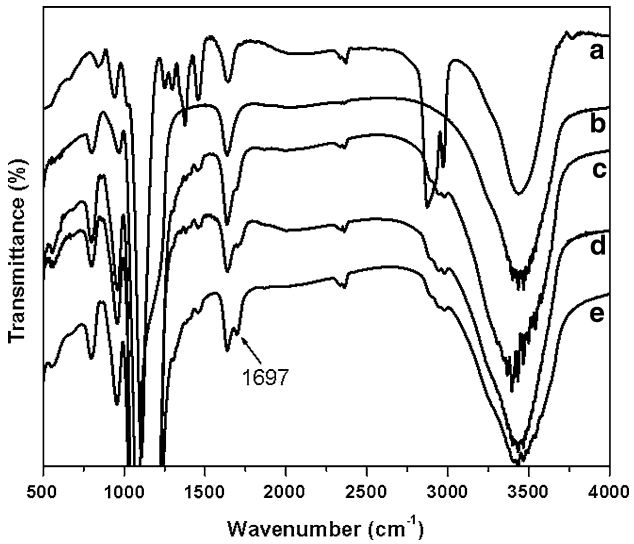

Fig. 5 IR spectrum of P123 (*a*), calcined SBA-15 (*b*), SBA-15/CO-5 (*c*), SBA-15/CO-7 (*d*), and SBA-15/CO-10 (*e*)

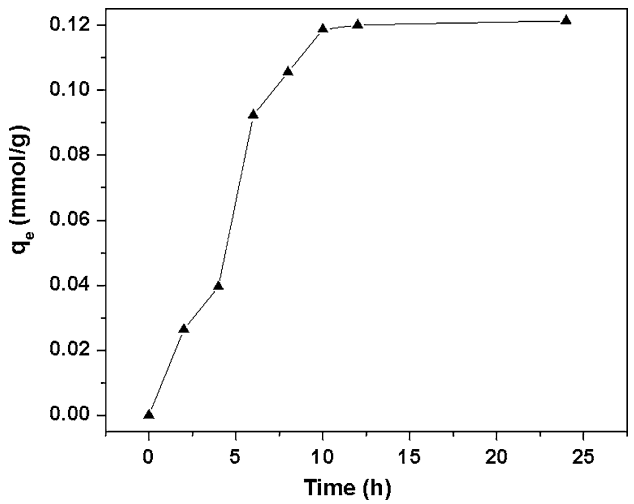

Fig. 6 Effect of contact time for the adsorption of phenol onto SBA-15/CO-10 with initial phenol concentration of 100 mg/L at 30 °C

samples are proportional to the TSPM contents in the initial mixtures Fig. 5.

3.2 Phenol adsorption

3.2.1 Adsorption equilibrium time

To investigate on phenol adsorption on the functionalized-materials, the experiments were carried out on a representative sample, SBA-15/CO-10. To obtain the equilibrium time of adsorption at 30 °C, liquid-phase adsorption experiments were conducted on solutions containing initial different concentrations of phenol in the presence of the adsorbent. Each solution was collected and analyzed at a different time. As shown in Fig. 6, for SBA-15/CO-10 with an initial phenol concentration of 100 mg/L, a burst adsorption was obtained within a contact time of 10 h after which adsorption was nearly unchanged. Equilibrium was reached at about 12 h. This adsorption equilibrium time was also obtained for the initial phenol concentrations of 50, 150, and 200 mg/L. However, we selected a stirring time of 24 h to obtain an absolute equilibrium for all subsequent adsorption experiments.

3.2.2 Adsorption isotherms

The isotherm for phenol adsorption of the SBA-15/CO-10 material is presented in Fig. 7. At low concentrations, the isotherm is linear, with it increasing more slowly at higher

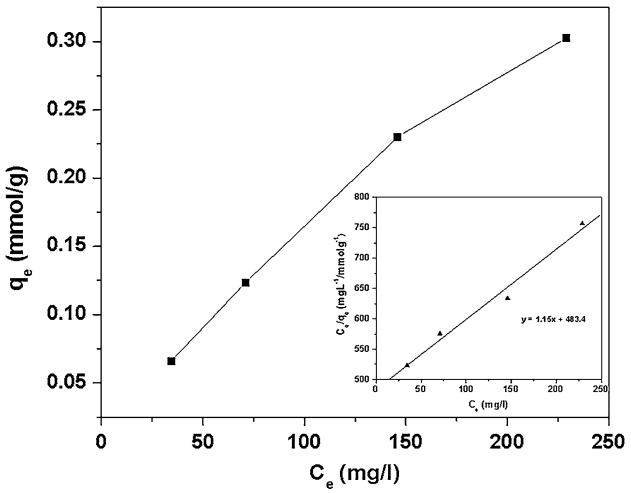

Fig. 7 The effect of initial concentrations and Langmuir plot (*the inset*) for the adsorption of phenol onto SBA-15/CO-10 at 30 °C

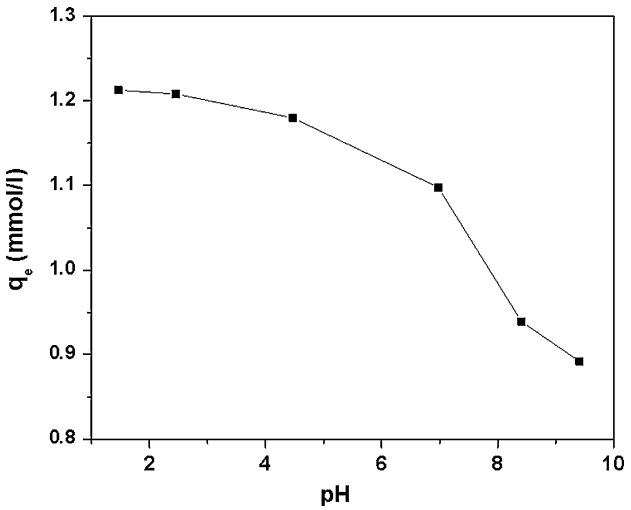

Fig. 8 Effect of pH for the adsorption of phenol onto SBA-15/CO-10 with initial phenol concentration of 100 mg/L at 30 °C

concentrations. The data for the adsorption were fitted to Langmuir Isotherms and the Langmuir linear plot is shown in Fig. 7. The maximum adsorption capacity of 0.87 mmol phenol/$g_{adsorbent}$ was also calculated from the linearized Langmuir equation.

3.2.3 Influence of Ph

The study on the influence of pH on the phenol adsorption capacity of SBA-15/CO-10 was performed at 30 °C and an initial concentration of phenol of 100 mg/L. We varied the initial solution pH values from about 2–10 and the results are shown in Fig. 8. It can be seen that the value of pH has a great influence on the adsorption property of the material for phenol. A decrease in uptake of phenol generally obtains for SBA-15/CO-10 with increasing the pH value from 2 to 10. However, the adsorption amounts decreased strongly at pH values over 7. This may come from different molecule forms of phenol. The form of hydrogen bond occurs possibly between carbonyl group with –OH of phenol. The dissociation degree of hydroxyl groups of phenol is enhanced with the increase of pH value, resulting in weakening hydrogen bond.

3.2.4 Regeneration of adsorbent

Desorption of phenol from phenol-loaded SBA-15/CO-10 was carried out by stirring for 2 h with acetone and ethanol solvents, individually. Then the solid phase was separated by filtration and investigated on adsorption of phenol again. Our results show that SBA-15/CO-10 can retain about 85 and 80% adsorption capacities for using acetone and ethanol eluents, respectively, after five consecutive operations. This result indicates that the material has good reusability.

4 Conclusion

The carbonyl-functionalized SBA-15 materials with various carbonyl contents have been synthesized and investigated for adsorption of phenol from aqueous solutions. The phenol adsorption approached equilibrium state in period of about 12 h. The adsorption data have been fitted to Langmuir isotherms and a maximum phenol loading of 0.87 mmol/g has been obtained for SBA-15/CO-10. pH has a great influence on the adsorption property of the material for phenol, and generally, a decrease in uptake of phenol obtained with increasing the pH value. The hydrogen bond between oxygen of carboxyl and hydrogen atoms of phenol plays an important role in the uptake of phenol on the materials.

Acknowledgments Financial support from the National Foundation for Science and Technology Development of Viet Nam (NAFOSTED, 104.03.06.09) is gratefully acknowledged.

References

1. Y. Ku, K.C. Lee, J. Hazard. Mater. **80**, 59 (2000)
2. J. Huang, X. Wang, Q. Jin, Y. Liu, Y. Wang, J. Environ. Manage. **84**, 229 (2007)
3. G. Buscaa, S. Berardinelli, C. Resini, L. Arrighi, J. Hazard. Mater. **160**, 265 (2008)
4. N. Ahalya, T.V. Ramachandra, R.D. Kanamadi, Res. J. Chem. Environ. **7**, 71 (2003)
5. S. Mukherjee, S. Kumar, A.K. Misra, M. Fan, Chem. Eng. J. **129**, 133 (2007)
6. A. Tor, Y. Cengeloglu, M.E. Aydin, M. Ersoz, J. Colloid Interface Sci. **300**, 498 (2006)

7. S. Rengaraj, S. Moon, R. Sivabalan, B. Arabindoo, V. Murugesan, J. Hazard. Mater. **89**, 185 (2002)
8. H.B. Senturka, D. Ozdesa, A. Gundogdua, C. Durana, M. Soylakb, J. Hazard. Mater. **172**, 353 (2009)
9. D. Zhao, J. Feng, Q. Huo, N. Melosh, G.H. Fredrickson, B.F. Chmelka, G.D. Stucky, Science **279**, 548 (1998)
10. D. Zhao, Q. Huo, J. Feng, B.F. Chmelka, G.D. Stucky, J. Am. Chem. Soc. **120**, 6024 (1998)
11. S. Dai, M.C. Burleigh, Y.H. Ju, H.J. Gao, J.S. Lin, S.J. Pennycook, C.E. Barnes, Z.L. Xue, J. Am. Chem. Soc. **122**, 992 (2000)
12. J. Brown, L. Mercier, T.J. Pinnavaia, Chem. Commun. 69 (1999)
13. C.P. Jaroniec, A. Sayari, M. Kruk, M. Jaroniec, J. Phys. Chem. B **102**, 5503 (1998)
14. V. Antochshuk, M. Jaroniec, J. Phys. Chem. B **103**, 6252 (1998)
15. A. Walcarius, L. Mercier, J. Mater. Chem. **20**, 4478 (2010)
16. A.S.M. Chong, X.S. Zhao, J. Phys. Chem. B **107**, 12650 (2003)
17. J. He, Y. Xu, H. Ma, D.G. Evans, Z. Wang, X. Duan, Microporous Mesoporous Mater. **94**, 29 (2006)
18. K. Moller, T. Bein, R.X. Fischer, Chem. Mater. **11**, 665 (1999)